The International Journal of Advanced Manufacturing Technology (2019) 105:4773–4782
https://doi.org/10.1007/s00170-019-04558-5

ORIGINAL ARTICLE

High-accuracy and high-performance WAAM propeller manufacture by cylindrical surface slicing method

Tianying He[1] · Shengfu Yu[1] · Yusheng Shi[1] · Yili Dai[1]

Received: 3 April 2019 / Accepted: 2 October 2019 / Published online: 16 November 2019

Abstract
The propeller is the important component of the power system in ships, the blades of which are spatial curved structures with continually changing sections. Wire arc additive manufacture (WAAM) is a novel technology and an effective method for manufacturing propellers. Currently, the planar slicing methods cannot form the high-accuracy propellers with complex spatial curves, a new cylindrical surface slicing method, based on the principles of conformal slicing, is applied to WAAM, the section for slicing being a cylindrical surface coaxial with the hub. Both cylindrical circumferential filling and cylindrical axial filling are used for filling the blades. In the manufacturing process, the hub is firstly formed by plane slicing and offset filling, then the blade is formed piece by piece by cylindrical slice and cylindrical axial filling and cylindrical circumferential filling alternately. A non-contact 3D measuring is conducted with a surface structure light 3D scanner after the completion of printing, and a 3D comparison is made with Geomagic qualify software. The dimensional error of the product is within ± 1.6 mm. The mechanical properties of WAAM propeller components are higher than the casting ones with the same composition.

Keyword Propeller · Wire arc additive manufacture · Cylindrical slicing · 3D measuring · Forming accuracy

1 Introduction

The propeller is one of the core components in the power systems of ships. Its structure and shape has significant impact on the performance of these systems. The propellers consisted of a hub and blades: The hub was a revolving body and the blades were usually featured with a spatially curved body with a variable cross section. Now, the marine propellers are manufactured by casting in normal practices; thus, the process involves mold making, melting materials, casting, and CNC machining, making the manufacturing process both time-consuming and expensive. Ma et al. studied optimization of casting process parameters for marine propellers; he found that defects such as shrinkage hole and cracks were likely to occur at the intersection of the blade and the hub [1]. Lee, S. and Lee, W. used thermomechanical finite-element analysis method to analyze thermal deformation of a large marine propeller casting during solidification [2]. They believed that the blade generated torsional deformation in the casting process. Therefore, it is not only long manufacturing cycle and expensive to manufacture propellers by casting, but also prone to quality problems of defects and deformation. In order to fabricate high-quality propellers, a new method must be used to manufacture the propeller.

Wire arc additive manufacture (WAAM) is a new technique in producing complex surface metal objects. It would first slice the component into layers and make a path plan according to the shape of the target. Then, with arcs introduced as the heat source, metal wires are melted and stacked layer by layer until the component is fully accumulated [3–5]. Williams et al. formed large curved metal components for aerospace using WAAM, including Ti-6Al-4V spars, aluminum wing rib models [6]. It demonstrates that WAAM can produce high-quality curved component. Ding researched using WAAM

✉ Shengfu Yu
yushengfu@hust.edu.cn

Tianying He
d201780309@hust.edu.cn

Yusheng Shi
shiyusheng@hust.edu.cn

Yili Dai
931583346@qq.com

[1] State Key Laboratory of Materials Processing and Die & Mould Technology, Huazhong University of Science and Technology, Luoyu Road, Wuhan 1037, China

technology to manufacture nickel aluminum bronze (NAB) components [7]. WAAM NAB parts without post-processing are fully dense and exhibit fine microstructure, as well as comparable mechanical properties, to as-cast NAB alloy. Dai et al. investigated the mechanical properties and microstructure of the WAAM high-building multi-directional pipe joint [8]. As he illustrated, the microstructure of the WAAM components is very compact, the grain size is small. Ma et al. used WAAM to deposit large-scale aluminum alloy thin-walled members, which proved that this technology has the advantage of high deposition rate, high energy efficiency, and low cost [9]. Li et al. proposed an adaptive process control scheme (APCS) capable to improve the accuracy of WAAM complex-shape components [10]. This illustrates that WAAM technique is an effective way to fabricate complex-shaped metal components. So, WAAM technology suitable for production of propellers with high-precision and excellent performance.

Propeller fabrication by WAAM process has attracted wide attention. Zhou et al. first adopted the WAAM technology to produce an equal-section surface block similar to blade, then milling it into the shape of a propeller blade [11]. WAAM technology is able to realize the forming of variable cross-section space curved surface. However, Zhou did not use a suitable path planning method to manufacture variable cross section propeller by WAAM. Ding et al. fabricated an 80 mm × 80 mm × 120 mm propeller with laser metal-wire additive manufacturing whose blade cross section is uniform and thin [12]. For this kind of propeller simulator with thin blade and equal cross section, it is not necessary to fill in the interior, but only need to form single contour in path planning. In fact, the thickness of marine propeller blade is constantly changing, so a reasonable path planning method must be researched to form variable cross section propeller. Ya et al. also used WAAM to form a propeller part [13]. However, the thickness and cross-section of abovementioned propeller parts are essentially constant. In fact, the propeller component is a curved body with variable cross section. The method mentioned above cannot be used for manufacturing variable cross-section propellers. In order to manufacture variable cross section propeller parts by WAAM technology, a slicing method and path planning method must be essential.

Most of the current WAAM process involves slicing the 3D model into a series of 2D planar contours with a constant or adaptive thickness perpendicular to the build-up direction [14]. Wu et al. studied an adaptive slicing algorithm for rapid prototyping (RP) techniques [15]. Although this algorithm improves the efficiency of slicing, it is often necessary to form extra supporting structures for complex components. Many 3D slicing methods have been focused on minimizing support structures. Ruan et al. proposed an automated slicing for a multi-axis metal deposition [16]. This slicing method can identify the centroid axis of different parts of component that want the central axis and slice along the axis. Ding et al. presented an algorithm based on a divide-and-conquer strategy, effectively reduced starting-stopping points and improved surface accuracy [17]. Wang et al. studied a slicing algorithm which can change the thickness and direction to manufacture large overhang structure without support [18]. These methods can effectively reduce the support structure when forming complex components. However, these slicing methods are based on the principle of plane slicing. For propeller components, the slicing path is discontinuous when the plane is used to slice the connection between blade and hub. In the WAAM processing, the arc striking or extinguishing frequently would affect the component accuracy and even at times ends up in deposition defects [19]. Therefore, in order to solve the problem of discontinuous path and multiple arcing caused by plane slicing, a new slicing method must be proposed to form propeller components by WAAM. At present, the common path planning methods are raster, zigzag, contour, spiral, and so on. [20]. Path planning is determined according to the slicing method. Therefore, it is necessary to study a new path planning method.

In order to improve the accuracy of the propeller fabricated by WAAM, reduce its defects, and solve the problems of discontinuous path and multiple extinguishing of the arc of plane slicing, a new slicing and path planning method is proposed. The method is used to manufacture the propeller components by WAAM, and the forming precision and performance of the propeller are studied and analyzed, which provides basic data for the manufacturing of the propeller components by arc material addition.

2 Experiment material and equipment

A 500 mm × 500 mm × 50 mm Q235 steel plate is used as the substrate. Printing material for this propeller wire arc additive manufacture is a metal wire called EH700-1, with a diameter of 1.2 mm. The wire is directly deposited under CMT arc heat. The composition of the wire and the deposited metal is shown in Table 1. Equipment used in the experiment include a CMT

Table 1 EH700-1 chemical composition (wt.%)

	C	Mn	Si	Cr	Ni	Ti	B
EH700-1	0.06–0.08	1.00–1.30	0.30–0.37	0.68–0.70	2.60–3.00	0.010–0.015	0.007–0.015
Deposition metal	0.07	1.17	0.33	0.69	3.20	0.013	0.007

Table 2 Parameters for WAAM propeller simulator

Current	Voltage	Speed	Gas
140 A	20 V	7–8 mm/s	100% CO_2

(cold metal transfer) arc welding power source and a KR30-HA robot. The propeller simulator was formed layer by layer using the wire arc additive manufacturing method.

Forming propeller simulator using the process parameters in Table 2. During the deposition process, the arc torch is always aligned to the normal vector of the pool surface. The single-pass deposition metal has a width of 7.4 mm and a height of 2 mm; therefore, multi-pass deposition was necessary to achieve required thickness.

When the deposition is finished, the propeller simulator is measured by a Powerscan 3D scanner in a non-contact manner to retrieve the 3D dot cloud file. Geomagic qualify point cloud analysis software is then used to fit and encapsulate the point cloud files. 2D and 3D comparison is conducted to obtain the deviation of the actual model from the idealized model. Samples are taken from the simulator model to perform mechanic tests, including tensile strength, yield strength, impact toughness, and elongation. Samples are also analyzed by both optical and scanning electron microscope (SEM) to determine the microstructure of the simulator.

3 Surface slicing algorithm and path planning

3.1 Modeling of the propeller

A propeller is made up of several blades and a hub. The blades were typical complex spatial curved surfaces whose section was constantly changing. The blueprint of a propeller contains a side view, a projected and expanded outlines, a maximum thickness distribution section shape, a profile offsets and geometry parameters of designed propeller, and so on. In the planar layout of a propeller, blade reference line is defined as the main lead in the center of the blade, as is shown in Fig. 1a, line OU. The angle θ between the blade reference line and the blade axis is called trim angle; Y_R the trim amount. Figure 1 c shows the stretched contour map which contains information like 0.2 R-0.9 R blade section, screw pitch, and distance from maximum thickness to the trailing edge.

In order to produce high-precision propeller components for WAAM, an accurate 3D model of the propeller must be created. The propeller blades are complex spatial surfaces. A high-precision propeller blade surface model thus must be obtained by fitting the feature points as shown in Fig. 1c. In accordance with the process shown in Fig. 2, an accurate model of the propeller is built in the 3D modeling software Unigraphics NX software developed by Siemens. To begin with, create a DAT format point cloud file with 3D coordinates provided by the feature points table; import the file to Unigraphics NX software and fit points of the same height with B-spline curve as well as smooth curves chain. Then, geometry transformation is performed. These transformations include rotation shift where the helix angles α are calculated by screw pitch, translation shift based on the trim amount Y_R and distance from maximum thickness to the trailing edge, and winding shift that winds the section curve to the respective heights of the cylinder. The last step is to form a "blade sheet" and eventually the blade entity via "sewing" the blade sheet, as in Fig. 3. It is saved as a propeller slice model in the STL file format in the Unigraphics NX software. It is well known that errors may occur in the STL file, which may result in inaccurate slicing paths and reduce the precision of the

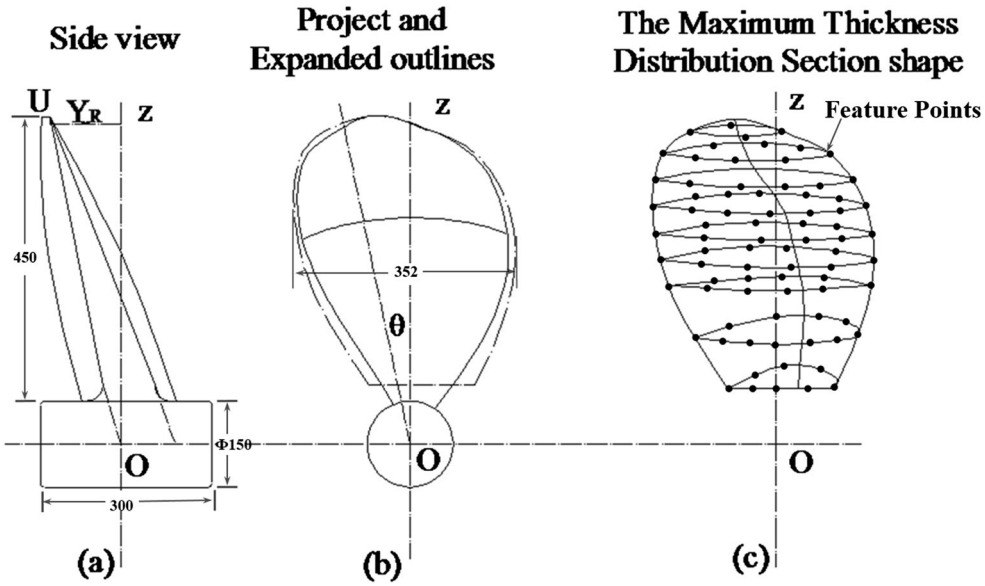

Fig. 1 **a**–**c** Propeller plane drawing

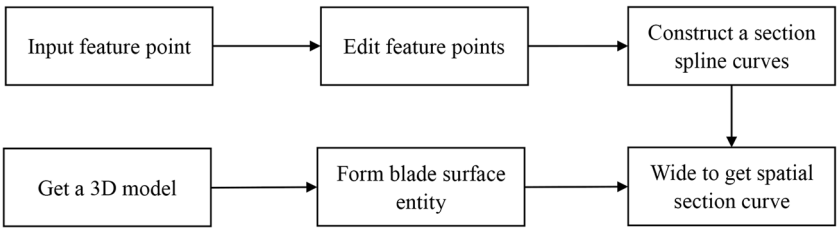

Fig. 2 Propeller modeling flow chart

WAAM propeller parts. Therefore, the exported propeller STL model must be checked and repaired. In this paper, the Magics software developed by Materialise is used to inspect and repair the propeller STL model, and the normal direction, holes, and gaps in the model are repaired. Through the repairing, a structurally correct propeller STL model is obtained.

According to the design requirements of the propeller in this paper, the blade has a total height of 450 mm, wherein the first 0–150 mm blade has a helix angle of 30°, the middle 150–300 mm has a helix angle of 20°, and the last 300–450 mm has a helix angle of 10°. The phenomenon that the helix angle being abrupt serves a special function. The geometrical characteristic of the propeller is the combination of complex blade surfaces and intricate intersection lines.

3.2 Cylindrical surface slicing method

After modeling, the blade is sliced by a cylindrical surface, which is coaxial with the hub and has the same radius as the outer surface of the hub. Its radius increases with the slice height, as shown in Fig. 4. The printing contour obtained by cylindrical surface slicing is the intersection line between the blade and the hub of the propeller. In this way, the printing path is a continuous space curve, which can avoid the problem that the printing path is discontinuous and multiple arcing when printing complex curved surface components. It greatly improves the accuracy of propeller components.

However, the common slicing software is mostly based on the principle of planar slicing, that is, using a plane to STL model for slicing and path planning. For propeller components, the slicing path is discontinuous when a plane is used to slice the connection between the blade and the hub. In WAAM processing, the frequent ignition and extinction of the arc would do harm to component accuracy. So, a cylindrical surface slicing program was written in JAVA language for fabricating propellers. Cylindrical surface slicing starts with a cylindrical surface with the same radius as the hub, and gradually raises the slicing height until the top of the blade. The height of lifting is the height of a single layer of deposition usually 2.5 mm. The printing path obtained by cylindrical surface slicing is implemented in the following steps:

(1) Define the cylindrical slicing surface. The axis of the cylindrical surface is defined by the coordinates of two points on the hub axis, and the radius of the cylindrical surface can be determined by the height of the slice.
(2) Determine the relative location of the cylinder surface and the triangle pieces in the STL model file. The triangle faces and their relations in dots, lines, and surfaces are stored in the STL model, and the overall topological relation is rooted on a binary tree. The relationship between adjacent triangles faces is defined. Through this relationship, adjacent triangle faces of arbitrary triangular faces can be located. In the meantime, these triangles are sorted by their location info. When the direction of a slice lifting direction is aligned with Z axis, the coordinate of three vertices will be recorded; they will be sorted

Fig. 3 Propeller simulator 3D model

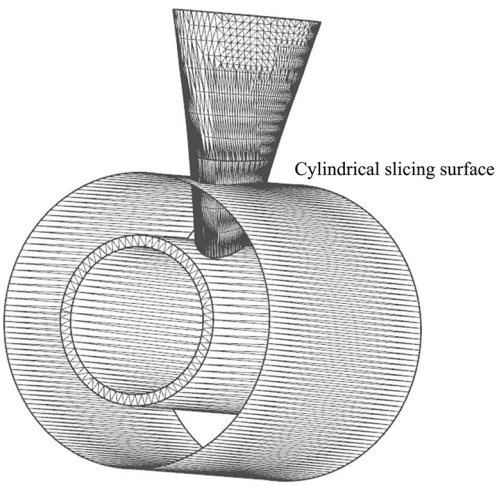

Fig. 4 Schematic diagram of cylindrical slicing surface

by their Z_{min}, and when Z_{min} are the same, the one with smaller Z_{max} will be put in the front. As the sorting coming to an end, the determination process is started. The intersected patches will be stored in a dynamic set.

(3) Find the intersecting point of triangle pieces and the cylinder. This is shown in Fig. 5a Suppose PP_1 is the foot point of P to OO_1 , then $\left|\overrightarrow{OO_1}\right| = R$;

$$A(X_1, Y_1, Z_1); B(X_2, Y_2, \uparrow Z_2); O(X_S, Y_S, Z_S); O_1(X_e, Y_e, Z_e);$$
$$\overrightarrow{AB} = (X_1{-}X_2, Y_1{-}Y_2, Z_1{-}Z_2); \overrightarrow{OO_1} = (X_s{-}X_e, Y_s{-}Y_e, Z_s{-}Z_e);$$

Since P is on line AB,

$$P = (X_1 + t \times (X_1{-}X_2), Y_1 + t \times (Y_1{-}Y_2), Z_1 + t \times (Z_1{-}Z_2));$$
$$\overrightarrow{PO} = \left(X_1 + t \times (X_1{-}X_2){-}X_s, Y_1 + t \times (Y_1{-}Y_2){-}Y_s, Z_1 + t \times \left(Z_1{-}Z_2\right){-}Z_s\right)$$

$$\cos\varphi = \frac{\overrightarrow{PO} \cdot \overrightarrow{OO_1}}{\left|\overrightarrow{PO}\right| \cdot \left|\overrightarrow{OO_1}\right|} \quad (1)$$

$$\sin\varphi = \frac{R}{\left|\overrightarrow{PO}\right|} \quad (2)$$

With formula (1) and (2), parameter t can be determined, giving us the coordinates of P. In turn, every intersecting point can be found.

There are two exceptional cases in the process of intersection: one is shown in Fig. 5b, as the triangle patch has only one intersecting point with the cylinder; under such a circumstance, the coordinates of this point should be stored. Another case is shown in Fig. 5b, as one side of the triangle is on the section. This side should be discarded, instead, the intersection of another two sides of the triangle and the cylinder should be stored.

(4) When the set in step (3) is completed, connect the dots in order to draw the outer contour printing path.

3.3 Path planning method of cylindrical surface slicing

Now that the inner and outer contour has been determined by the aforementioned methods, filling is required, quality of which will directly determine the accuracy of the propeller printing. In this article, two filling paths are experimented. When the deposition direction is along Z axis, it is possible to fill along X axis (circumferential direction) or along Y axis (axial direction). Respectively, the two means are defined as cylindrical circumferential filling and cylindrical axial filling.

Huang et al. proposed an error-tolerance slicing algorithm for STL files. It illustrated standard STL (stereolithography) files that consist of surface information in triangle patches, lacking inner entity information [21]. Therefore, the filling path cannot be obtained directly by cylindrical surface slicing. For the complex curve of propeller cross section, it is impossible to get the internal filling path gradually according to a certain offset. Because the curvature at both ends of the propeller section curve is very large, the intersection point will be generated at both ends when the offset inward, which will affect the filling quality.

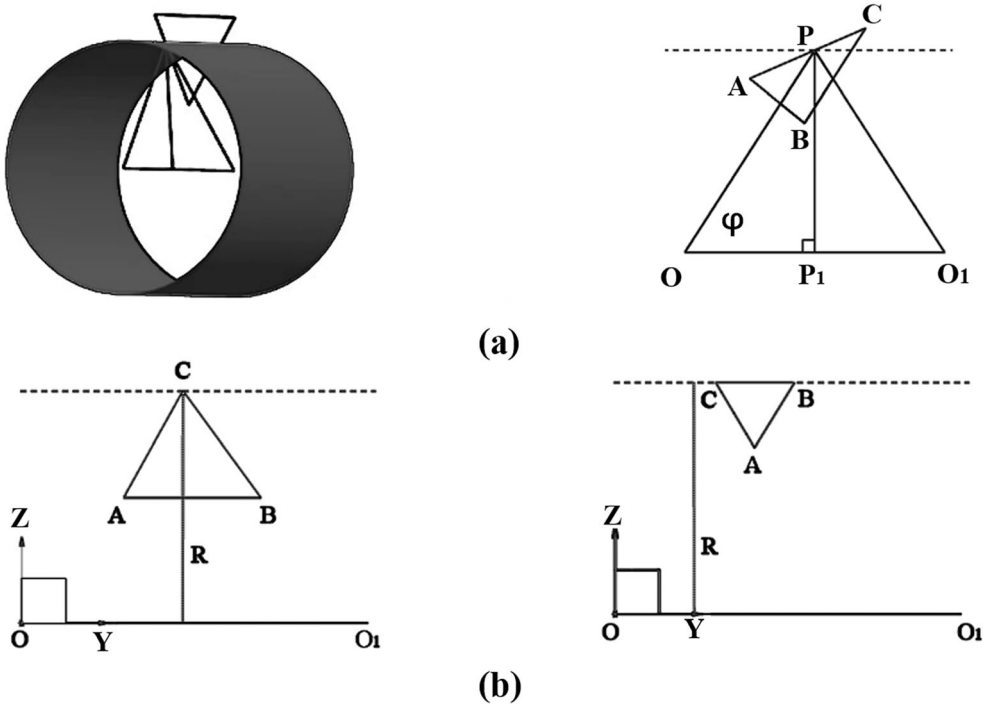

Fig. 5 **a**, **b** Schematic diagram of the intersection of a triangular faces and a cylindrical surface

In order to prevent this situation from occurring, the article proposes a method of the internal filling path of STL file surface slice: filling on the sliced cylinder with a uniform "grid," as shown in Fig. 6a. Unlike planar slices, the Z coordinates of data points of filling paths are not fixed values equal to the slice height, but a series of points distributed on the cylindrical surface when path planning of cylindrical surface slicing. Therefore, not only the X and Y coordinates of each filling path data point but also the Z coordinates of each point need to be calculated in the path planning.

(1) Cylindrical circumferential filling method

The offset of the cylindrical circumferential filling method is half the width of a single deposition, that is, 3.5 mm. According to the blade profile obtained from the cylindrical surface slicing, the X_{max} and X_{min} of the contour edge are calculated respectively. The filling path x_{fill} begins with X_{min} and increases by 3.5 mm each time until X_{max}. The coordinates of the outline data points are obtained from the cylindrical surface slices, and the coordinate ranges of the propeller contour corresponding to each x_{fill} in the Y direction are calculated respectively. They are recorded as y_1 and y_2; within the range of y_1 and y_2, mark every point every 3.5 mm and calculate corresponding Z coordinates for each point on the cylinder. Connect the dots with the same X coordinate in order, the circumferential filling path is set, as shown in Fig. 6b.

(2) Cylindrical axial filling method

Cylindrical axial filling is similar to cylindrical circumferential filling, the offset of which is 3.5 mm. According to the

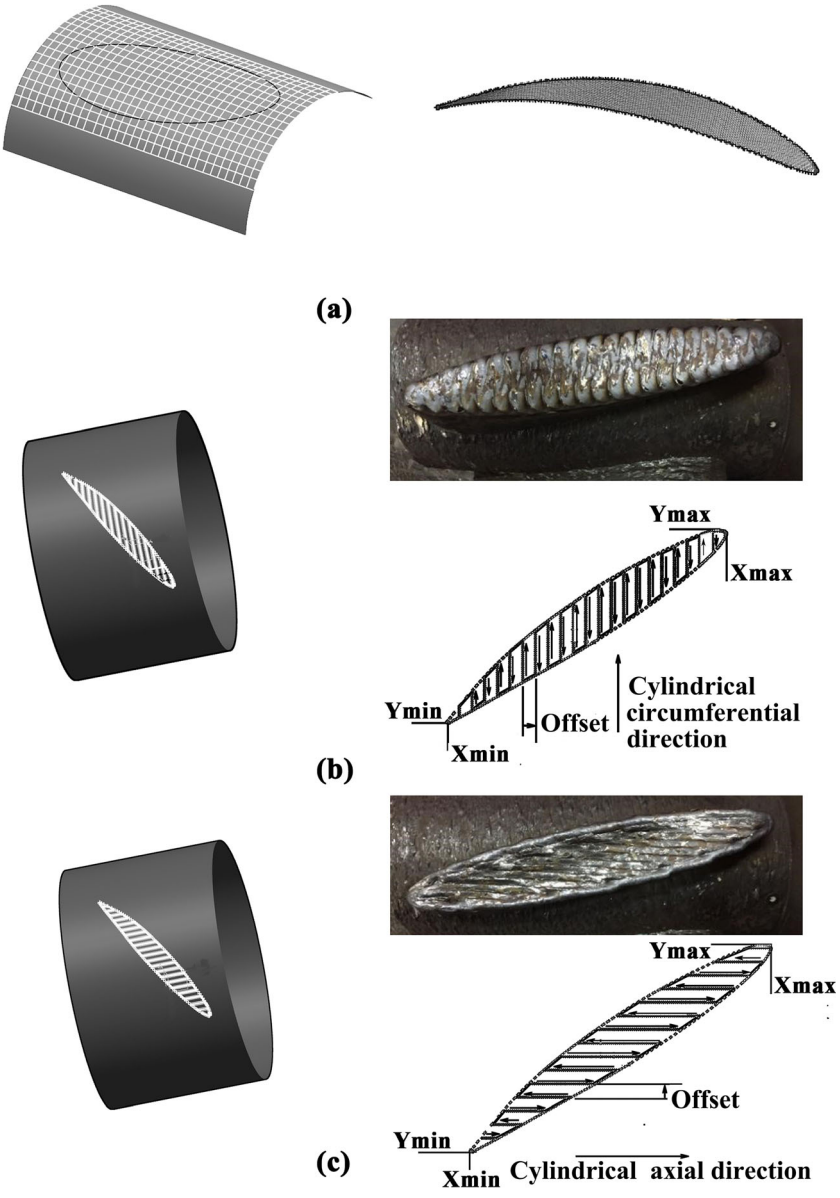

Fig. 6 Path planning. **a** Schematic diagram of the filling path calculation. **b** Schematic diagram of cylindrical circumferential filling. **c** Schematic diagram of cylindrical axial filling

blade profile obtained from the cylindrical surface slicing, the Y_{max} and Y_{min} of the contour edge are calculated respectively. The filling path y_{fill} begins with Y_{min} and increases by 3.5 mm each time until Y_{max}. The coordinates of the outline data points are obtained from the cylindrical surface slices, and the coordinate ranges of the propeller contour corresponding to each y_{fill} in the X direction are calculated respectively. The intersections are marked with x_1 and x_2; similarly, within the range of x_1 and x_2, mark every point every 3.5 mm and calculate corresponding Z coordinates for each point on the cylinder. Connect the dots with the same Y coordinate in order to set the surface axial filling path as shown in Fig. 6c.

In the actual calculation process, the point in the filling path that coincides with the contour path needs to indent to the inside of the contour by 3.5 mm to avoid interference from the filling path and contour. Meanwhile, the overlap ratio needs to be ensured during actual accumulation.

4 Propeller simulator manufacture

4.1 Deposition process and results

Before the actual printing, the simulator needs to be divided into several regions: one for the hub and one for each blade for the complexity and symmetry of the blade. In the manufacturing process, the hub is first formed by plane slicing and offset filling, and the blade is formed piece by piece by cylindrical slice and cylindrical axial filling and cylindrical circumferential filling alternately. The alternating of the two filling methods can ensure the isotropy of the mechanical properties of the propeller simulating blades.

Since the hub and the cylindrical surface are coaxial, the hub, in the paper, is manufactured first; the blades are later printed on the hub piece by piece. Kazanas et al. researched the fabrication of geometrical features using WAAM and described the dimensional error of component due to heat accumulation [22]. For reducing the effect of heat accumulation on the contour dimensional accuracy, the inner part is firstly formed and then the contour is printed layer by layer. The cylindrical axial filling is as shown in Fig. 6b, the cylindrical circumferential filling is as shown in Fig. 6c, and the actual deposition result is as shown in Fig. 7.

4.2 Dimensional error of the propeller

Powerscan is a non-conducting 3D scanner based on surface structured light, whose measurement accuracy can reach ± 0.05 mm and single plot cloud scan can reach 0.5 s. In the process of producing propeller simulator with WAAM, 8–10 photos of point cloud file are taken along the predetermined trajectory. These files are auto-stitched; then, high-precision point cloud files of propeller simulator are prepared.

Fig. 7 Deposition results

Post-processing is a necessary step to obtain the actual 3D model of the propeller. Point cloud files are imported into Geomagic qualify. 3D model after packaging, patching, and smoothing is shown in Fig. 8. Target propeller model created by UG is in Fig. 3.

A comparative analysis is performed after point cloud file fitting. The specific steps are listed as follows: (1) Import the scanned model into Geomagic qualify software as the testing object and import the target model as the reference object. The target model is defined as point cloud M_1, and the scanned model is defined as point cloud N_1. (2) Use the "four-point method" to roughly align the two cloud files.

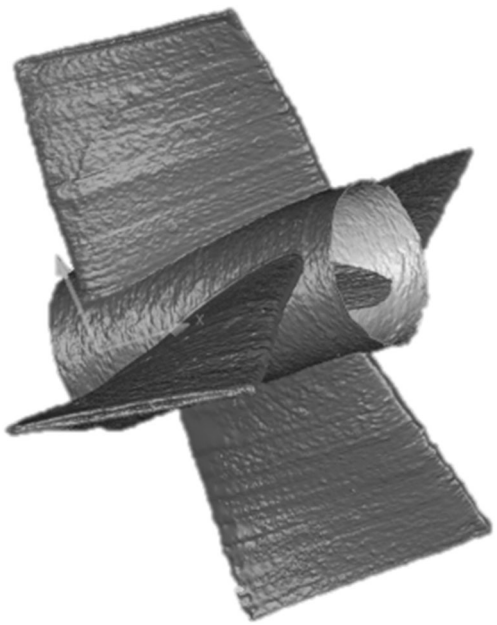

Fig. 8 Propeller actual 3D measurement model

Select four feature points on N_1, which form a feature point pair with four feature points at the corresponding position on M_1, as is shown in Fig. 8. And the rotation matrix S_1 and translation matrix T_1 between M_1 and N_1 are calculated by using the feature point pairs. Rotate and translate N_1 in Geomagic qualify software. (3) Use the "iterative closest point (ICP)" method to get the accurate alignment of the two cloud files. For each point in N_1, find the closest point in M_1 and record the two points as associated point pairs. The rotation matrix S_2 and the translation matrix T_2 between the two cloud files are calculated using the associated point pairs. After N_1 is rotated and translated, the average relative distance of all associated point pairs is calculated and recorded as M, as is shown in formula (3).

$$M = \sum_{i=0}^{n} \sum_{j=0}^{m} \left[\left(S_i \times N_{1j} + T_i \right) - M_{1j} \right] \quad (3)$$

Conduct the iteration until the average relative distance M is less than the set threshold of 0.1 mm. Finally, the rotation matrices S and T between the two cloud files are obtained. Rotate and translate N_1 in the Geomagic software. (5) When alignment is finished, the test object and the reference object enter the comparison phase. 3D, 2D, and boundary comparison will be conducted.

In this paper, 3D comparison is conducted to measure the overall dimension error; 2D comparison to measure the error in different sections. The results are in Fig. 9. From the deviation chromatography in Fig. 9a, it is obvious that there is some deviation in the blades with curved section planning path. The average error is ± 1.6 mm. The single blade error is shown in Fig. 9b, and the average error is ± 0.95 mm.

The deviation distribution histogram of a single blade is shown in Fig. 9c. The deviation between the actual model and the target model of a single blade is 18.34% distributed in

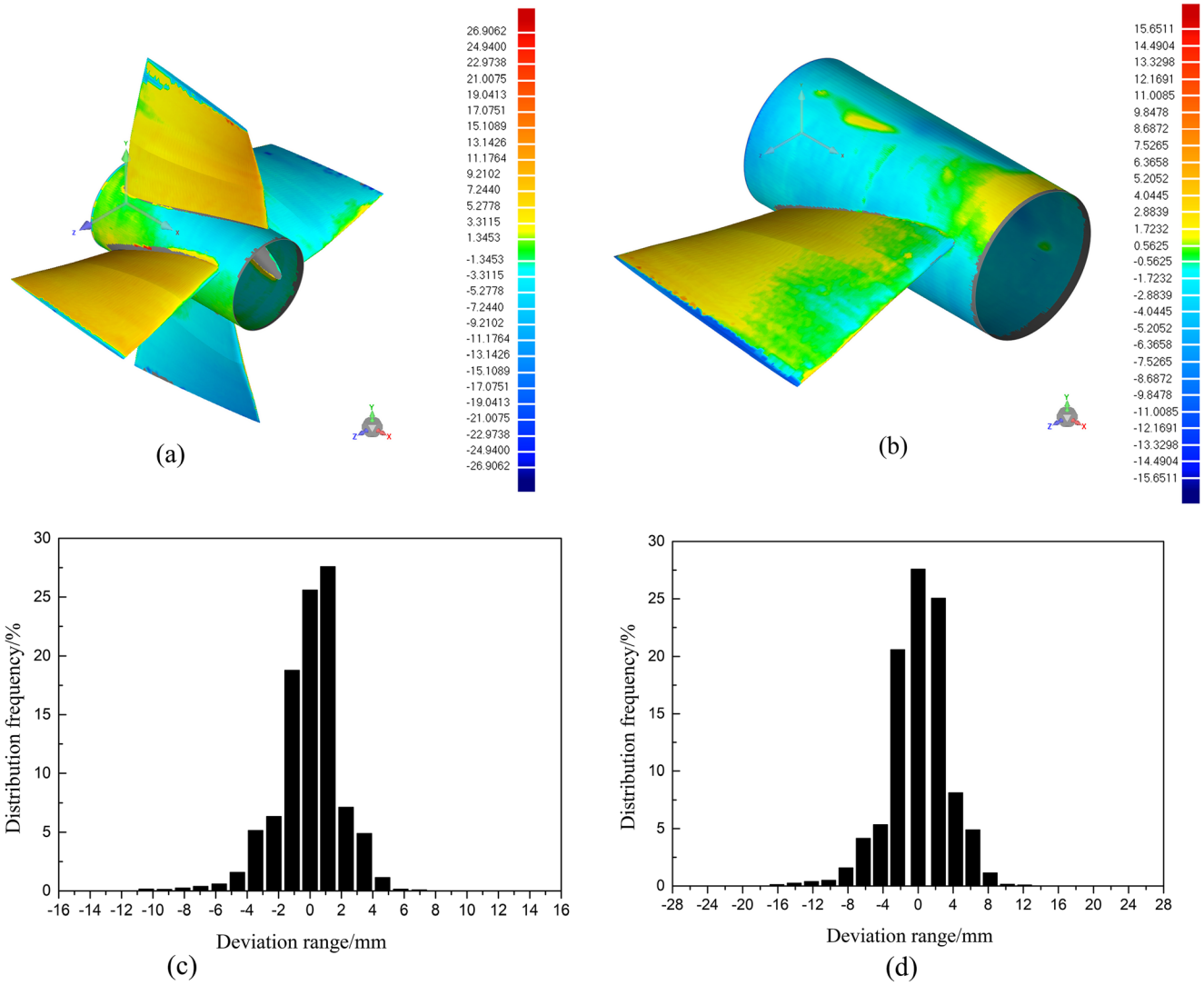

Fig. 9 Schematic diagram of error analysis. **a** Overall error analysis. **b** Single blade error analysis. **c** Histogram of propeller overall deviation distribution. **d** Histogram of single blade deviation distribution

Table 3 Mechanical property measurement results

Material	Tensile strength (σ_b/MPa)	Yield strength ($\sigma_{0.2}$/MPa)	Elongation (δ/%)	Impact toughness (− 20 °C)/J	HB
Casting propeller	≥ 700	≥ 500	≥ 16	≥ 40	≥ 240
WAAM propeller	758	523	21	53	242
Increasing rate (%)	8.3	3.8	31.2	32.5	0.8

the range of ± 0.56 mm, 22.47% in the range of − 1.72 to − 0.56 mm, and 17.77% in the range of 0.56–1.72 mm. A total of 82.43% is distributed within the range of ± 2.88 mm. The average error of the propeller blades is ± 0.95 mm, and the accuracy of the blades meets the design requirements. As is shown in Fig. 9d, the overall deviation distribution histogram of the propeller parts, the deviation between the actual propeller model and the target model is 27.58% in the range of ± 1.35 mm, 20.59% in the range of − 3.31–1.35 mm, and 25.04% in the range of 1.35–3.31 mm. A total of 73.21% is distributed in the range of ± 3.31 mm. Because the four blades on the hub have slight deformation, the overall accuracy is slightly lower than the accuracy of the single blade, but the overall accuracy of the propeller component still meets requirement.

The dimensional accuracy of propellers made with WAAM is decided by the process parameters and the accuracy of the single cladding layer. In the forming process, the process parameters can be adjusted according to the size of the propeller in real-time three-dimensional measurement, thereby more effectively controlling the dimensional accuracy of the propeller. Furthermore, the arc is extremely unstable during the arcing and quenching phase, which will enlarge the dimensional accuracy error in a single cladding layer. In this paper, the cylinder surface slicing method is adopted, and path planning is designed accordingly, which aims to reduce arcing and quenching frequency and increase the accuracy of the single cladding layer. In the meantime, during the deposition process, the arc gun follows the normal vector direction of the molten pool surface, the arc force does not increase the flow tendency of the liquid pool on the cylindrical surface, being beneficial to the dimensional accuracy. All these contribute to the high precision of WAAM.

Ultrasonic flaw detection is deployed to perform a non-destructive inspection. Porosity and cracks are rarely found in the simulator, indicating the quality meets the standard.

4.3 Microstructure and mechanical properties of propeller simulator

Tensile and impact tests were carried out at room temperature. The test results are shown in Table 3. It can be clearly seen that the tensile strength of the WAAAM propeller is 8.2% higher than that of the casting, the yield strength increases by 3.8%, the elongation raises 31.2%, the Brinell hardness is basically the same, and the impact toughness improves more than 30%. The mechanical properties of the propeller simulator meet the requirements.

The optical structure of the propeller hub is shown in Fig. 10a, and the optical structure of the propeller blade is shown in Fig. 10b. The microstructure of the propeller being ferrite and granular bainite. Metallographic photographs were analyzed with Image pro plus. The average grain size does not exceed 15 μm. As we know, the smaller the grain size was, the higher the strength and toughness of the parts. Since the grain size of the propeller is approximately 15 μm, the strength and toughness of the propeller are very excellent.

5 Conclusions

(1) The cylindrical surface slicing method, which is based on the principle of conformal slicing, used a cylinder surface coaxial with the hub to slice the propeller blades and to

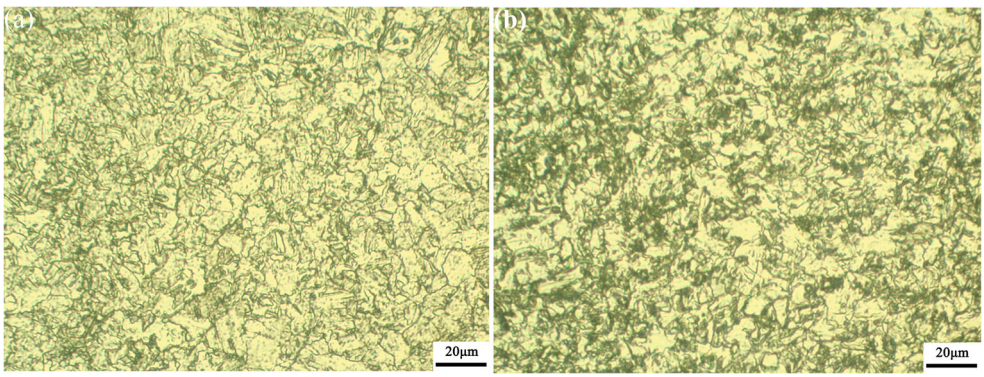

Fig. 10 Microstructure of WAAM propeller. **a** The hub. **b** The blade

plan the path. The method is proposed to form the complex surface structure of propeller.

(2) Two different filling methods are proposed for cylindrical surface slicing method, namely cylindrical circumferential filling and cylindrical axial filling. During the manufacture of the propeller by WAAM, the alternation of the two filling methods ensures the uniformity of the propeller mechanical properties.

(3) The dimensional error of the propeller simulator produced by the cylindrical surface slicing method is higher. The overall error of the propeller simulating parts is ± 1.6 mm, the error of the single blade is ± 0.95 mm, and the error of the blade section is ± 0.37 mm. The propeller forming accuracy meets the requirements.

(4) The mechanical properties of WAAM propeller components are higher than the casting ones with the same composition.

Funding information This work was supported by the National Key R&D Program of China, No. 2017YFB1103200, and Independent Innovation Fund of Huazhong University of Science and Technology, No. 2018KFYXMPT002.

References

1. Ma C, Chen N, Zhu YM, Li QF (2016) Simulation and optimization of casting process for marine helical blade. J Foundry Technol 5: 1058–1061
2. Lee SM, Lee WJ (2005) Finite-element analysis on thermomechanical behavior of a marine propeller casting in the sand-casting process. J Mater Eng Perform 3:388–394
3. Panchagnula JS, Simhambhatla S (2018) Manufacture of complex thin-walled metallic objects using weld-deposition based additive manufacturing. Robot Comput Integr Manuf 49:194–203
4. Li F, Chen SJ, Shi JB (2019) In-process control of distortion in wire and arc additive manufacturing based on a flexible multi-point support fixture. Sci Technol Weld Join 24(1):36–42
5. Geng H, Xiong J, Huang D et al (2017) A prediction model of layer geometrical size in wire and arc additive manufacture using response surface methodology. Int J Adv Manuf Technol 93(1):175
6. Williams SW, Martina F, Addison AC, Ding J, Pardal G, Colegrove P (2016) Wire + arc additive manufacturing. J Mater Sci Technol 7: 641–647
7. Ding D, Pan Z, Stephen VD, Shen C (2016) Fabricating superior NiAl bronze components through wire arc additive manufacturing. Materials 9(8):652–663
8. Dai Y, Yu S, Shi Y, He T, Zhang L (2018) Wire and arc additive manufacture of high-building multi-directional pipe joint. Int J Adv Manuf Technol 7:1–8
9. Ma G, Zhao G, Li Z, Yang M, Xiao WL (2019) Optimization strategies for robotic additive and subtractive manufacturing of large and high thin-walled aluminum structures. Int J Adv Manuf Technol 101:1275
10. Li F, Chen S, Wu Z, Yan ZH (2018) Adaptive process control of wire and arc additive manufacturing for fabricating complex-shaped components. Int J Adv Manuf Technol 96:871
11. Zhou HJ (2012) Research on complex impeller deposition & milling manufacturing. Huazhong University of Science &Technology
12. Ding Y, Akbari M, Kovacevic R (2018) Process planning for laser wire-feed metal additive manufacturing system. Int J Adv Manuf Technol 95:355–365
13. Ya W, Hamilton K (2018) On-demand spare parts for the marine industry with directed energy deposition: propeller use case. In: Meboldt M, Klahn C (eds) Industrializing Additive Manufacturing - Proceedings of Additive Manufacturing in Products and Applications - AMPA2017. AMPA 2017. Springer, Cham
14. Zhang YM, Chen Y, Li P, Male AT (2003) Weld deposition-based rapid prototyping: a preliminary study. J Mater Process Technol 135(2-3):347–357
15. Wu YF, Wong YS, Loh HT, Zhang YF (2004) Modelling cloud data using an adaptive slicing approach. Comput Aided Des 36(3):231–240
16. Ruan JZ, Eiamsa K, Liou FW (2008) Automatic process planning and toolpath generation of a multiaxis hybrid manufacturing system. J Manuf Process 7(1):57–68
17. Ding D, Pan Z, Cuiuri D, Li HJ (2014) A tool-path generation strategy for wire and arc additive manufacturing. Int J Adv Manuf Technol 73:173–183
18. Wang X, Zhang H, Wang G (2016) Adaptive slicing for waam to fabricate large overhang without support. J Huazhong Univ Sci Technol 1:56–59
19. Wang X, Wang A, Li Y (2019) A sequential path-planning methodology for wire and arc additive manufacturing based on a water-pouring rule. Int J Adv Manuf Technol 103:3813
20. Pan Z, Ding D, Wu B, Cumini D, Li HJ, Norrish J (2018) Arc welding processes for additive manufacturing: a review transactions on intelligent welding manufacturing
21. Huang SH, Zhang LC, Han M (2002) An effective error-tolerance slicing algorithm for STL files. Int J Adv Manuf Technol 20(5): 363–367
22. Kazanas P, Deherkar P, Almeida P, Lockett H, Williams S (2012) Fabrication of geometrical features using wire and arc additive manufacture. J Pro Inst Mech Eng B J Eng Manuf 226(6):1042–1051